DOI: 10.1002/ejic.201100284

Synthesis, Structure, and Thermoelectric Properties of Barium Copper Polychalcogenides with Chalcogen-Centered Cu Clusters and Te_2^{2-} Dumbbells

Oottil Mayasree,[a] Cheriyedath Raj Sankar,[a] Yanjie Cui,[a] Abdeljalil Assoud,[a] and Holger Kleinke*[a]

Dedicated to Professor John D. Corbett on the occasion of his 85th birthday

Keywords: Zintl phases / Solid-state structures / Sulfur / Selenium / Tellurium

$BaCu_{6-x}STe_6$ and $BaCu_{6-x}Se_{1-y}Te_{6+y}$ were synthesized from the elements at 663 K. These chalcogenides adopt a new structure type, cubic space group $Pm\bar{3}$, with a = 6.9680(2) Å in the case of $BaCu_{5.93}SeTe_6$. Therein, the Cu atoms form cubic clusters, centered by Se atoms, where statistically 2.07 corners are unoccupied. All Te atoms are part of Te_2^{2-} dumbbells, leading to a charge-balanced formula when x = 0: $Ba^{2+}(Cu^+)_6Se^{2-}(Te_2^{2-})_3$. While Te atoms can be incorporated on the Se site, no evidence was found for the ability of Se atoms to replace Te in the Te_2^{2-} pairs. Band structure calculations on different $BaCu_6SeTe_6$ models revealed a very small band gap at the Fermi level; all these chalcogenides with $x > 0$ should thus be *p*-doped semiconductors, which we experimentally confirmed for $BaCu_{5.7}Se_{0.6}Te_{6.4}$.

Introduction

Many chalcogenides form the backbone of various technologies encompassing rechargeable batteries[1] and the thermoelectric energy conversion[2–4] as well as technologies based on fast-ion conductors and phase-change materials.[5–7] This includes polysulfides in lithium-sulfur batteries[8] as well as polytellurides in thermoelectrics, for example $HfTe_5$ and Te_2^{2-} dumbbells,[9] and in *pnp*-junctions, such as the phase-change material $Ag_{10}Te_4Br_3$.[10]

In recent years, we have uncovered several new polychalcogenides by using barium and copper or silver as cations, including $Ba_2Ag_4Se_5$ with its linear Se_3^{4-} unit,[11] $Ba_3Cu_{14-x}Te_{12}$ with Te_2^{2-} dumbbells,[12] $Ba_{6.76}Cu_{2.42}Te_{14}$ with V-shaped Te_3^{2-} units,[13] and most recently $Ba_2Cu_{4-x}Se_yTe_{5-y}$, a mixed selenide-telluride with linear Te atom chains.[14] In the latter case, two different structures exist, depending on whether Se is incorporated into the structure. All examples with Cu exhibit significant deficiencies on the Cu sites (i.e., $x > 0$). $Ba_2Ag_4Se_5$ may be regarded as a typical (transition metal) Zintl compound,[15–18] wherein Ba and Ag formally transfer valence electrons to Se, which in turn attains its octet by formation of Se–Se bonds. Therefore, $Ba_2Ag_4Se_5$ is an intrinsic semiconductor according to $(Ba^{2+})_2(Ag^+)_4Se_3^{4-}(Se^{2-})_2$, as confirmed experimentally.[11] The same is true for $Ba_3Cu_{14-x}Te_{12}$ when x = 0, as implied with the charge-balanced formulation $(Ba^{2+})_3(Cu^+)_{14}(Te_2^{2-})_2(Te^{2-})_8$. For $x > 0$, $Ba_3Cu_{14-x}Te_{12}$ was thus predicted to be a *p*-doped semiconductor, in agreement with the physical property measurements.[12]

Using two different chalcogen atoms may lead to the formation of new structure types, as demonstrated recently with the structures of $Ba_2Cu_{4-x}Se_yTe_{5-y}$,[14] $Ba_3Cu_{17-x}Se_yTe_{11-y}$,[19] $Ba_2Cu_{6-x}STe_4$ and $Ba_2Cu_{6-x}Se_yTe_{5-y}$,[20] and $Ta_{15}Si_2Se_yTe_{10-y}$.[21] Here we present the new, isostructural, electron-deficient Zintl phases $BaCu_{6-x}Q_{1-y}Te_{6+y}$ with Q = S and Se, containing the above-mentioned Te_2^{2-} dumbbells.

Results and Discussion

Crystal Structure

The title compounds, $BaCu_{6-x}STe_6$ and $BaCu_{6-x}Se_{1-y}Te_{6+y}$, are isostructural, crystallizing in the cubic space group $Pm\bar{3}$ with one formula unit per unit cell. In the following, we will focus on the structure of $BaCu_{5.93(2)}SeTe_6$ as a representative of this series with a typical Cu deficiency of x = 0.07(2) and without Se/Te mixed occupancies.

The crystal structure of $BaCu_{5.9}SeTe_6$ is composed of $CuSeTe_3$ tetrahedra, which share common edges and corners to form a three-dimensional network. Each Te atom is connected to four Cu atoms as well as another Te atom in the form of a square pyramid, while each Se atom is situated in a cube formed by Cu atoms (left part of Figure 1). It should be noted that at least two Cu positions per unit

[a] Department of Chemistry, University of Waterloo, N2L 3G1 Waterloo, Ontario, Canada
Fax: +1-519-746-0435
E-mail: kleinke@uwaterloo.ca

Supporting information for this article is available on the WWW under http://dx.doi.org/10.1002/ejic.201100284.

cell are unoccupied in the case of hypothetical *BaCu6SeTe6* (occupancy of the Cu site: 75%), and thus statistically 2.07(2) in the case of $BaCu_{5.93(2)}SeTe_6$. There are three different possibilities to remove two Cu atoms from the $SeCu_8$ cube, as discussed below.

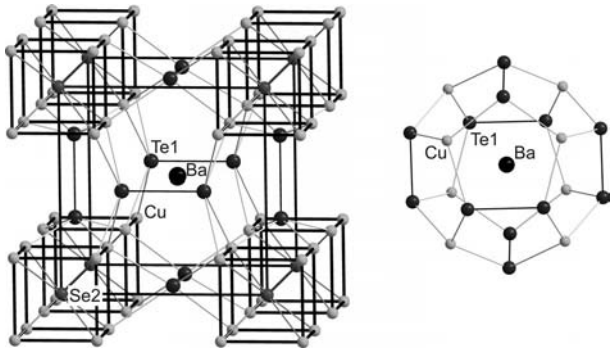

Figure 1. Left: crystal structure of $BaCu_{5.93(2)}SeTe_6$; right: its Ba-centered Cu_8Te_{12} pentagonal dodecahedron.

Assuming full Cu occupancy, the Ba atoms are located in a pentagonal dodecahedral Cu_8Te_{12} cage comprising twelve planar Cu_2Te_3 pentagons (right part of Figure 1). With Cu^+, this cage is best described as a Ba^{2+}-centered $[Cu_8(Te_2)_6]^{4-}$ anion. These dodecahedra are interconnected in all three directions via common edges formed by the Te_2^{2-} dumbbells.

The dodecahedron observed here is reminiscent of the $Ti_8C_{12}^+$ cation,[22] and topologically equivalent to the Cu_8Te_{12} cages occurring in $K_4Cu_8Te_{11}$,[23] $A_3Cu_8Te_{10}$, $A_2A'Cu_8Te_{10}$, and $A_2BaCu_8Te_{10}$ (A, A' = K, Rb, Cs).[24] These cages are interconnected by sharing of the ditelluride groups to infinite chains in case of $K_4Cu_8Te_{11}$ and to layers in the other cases. Thus, $BaCu_{5.9}SeTe_6$ is the first example with a three-dimensional connection of these dodecahedra, where all Te_2^{2-} entities are symmetrically equivalent. It is also the first example with the ideal T_h point group of the polyhedron. Finally, it is the only case among these cage compounds with a deficiency on the Cu site(s).

As a consequence of the encapsulation of the Ba atom in this cage, the coordination number of Ba, 12, is large. Correspondingly, the Ba–Te distance of 3.75 Å in $BaCu_{5.9}SeTe_6$ is larger than that in most Ba-Cu tellurides with a typical coordination number of nine and Ba–Te bonds in part shorter than 3.5 Å.[12,14] Slight variations of the Ba–Te bonds in the title compounds from 3.76 to 3.73 Å are possible, as replacing part of the Se atoms with Te increases the unit cell size, while replacing all Se atoms with S decreases it (Table 1). Equivalent Ba–Te distances of 3.74 Å on average occur in the (distorted) dodecahedra of $K_2BaCu_8Te_{10}$ and $Cs_2BaCu_8Te_{10}$.[24]

The other distances within the Cu_8Te_{12} cage are inconspicuous, with Cu–Te bonds around 2.61 Å and Te–Te bonds around 2.79 Å, the latter being indicative of a single bond, supporting the classification as Te_2^{2-} dumbbells. For comparison, the Te–Te bonds in such units are 2.78 Å in Rb_2Te_2[25] and 2.74 Å in $[N(CH_3)_4]_2Te_2$,[26] and they range from 2.77 to 2.86 Å in $K_2BaCu_8Te_{10}$ and $Cs_2BaCu_8Te_{10}$.

Table 1. Selected interatomic distances (Å) of $BaCu_{6-x}Q_{1-y}Te_{6+y}$.

Interaction	$BaCu_{5.7}Se_{0.5}Te_{6.5}$	$BaCu_{5.9}SeTe_6$	$BaCu_{5.9}STe_6$
Ba–Te1 12×	3.7625(2)	3.7515(1)	3.7332(3)
Cu–Q2 1×	2.4228(7)	2.4060(6)	2.3337(5)
Cu–Te1 3×	2.6152(3)	2.6102(2)	2.6104(3)
Cu–Cu 3×	2.7976(9)	2.7782(7)	2.6947(6)
Te1–Te1 1×	2.7895(6)	2.7826(4)	2.7875(4)

On the other hand, it is unusual that the Se site should be encapsulated in an Cu_8 cube in $BaCu_{5.9}SeTe_6$ with formally eight Cu–Se bonds of 2.41 Å, even when considering that about 25% of the Cu sites are unoccupied, that is, roughly 2 out of 8. Three symmetrically inequivalent $SeCu_6$ polyhedra are possible. The first one may be envisioned after removing two neighboring Cu atoms of the cube, resulting in space group *Pm* when retaining the same unit cell. The second one results when removing two Cu atoms along one face-diagonal, giving space group *P*2, and the third by removing two Cu atoms along one space-diagonal, yielding space group $R\bar{3}$ (Figure 2).

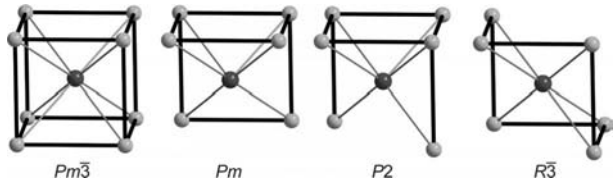

Figure 2. Different possible $SeCu_6$ clusters resulting from removing two corners from the $SeCu_8$ cube. The space groups are given for the $BaCu_6SeTe_6$ models with such clusters.

Noting that the cube edges are only 2.78 Å in $BaCu_{5.9}SeTe_6$ and can be as short as 2.69 Å in $BaCu_{5.9}STe_6$, the existence of Cu–Cu bonds is likely. Such bonds between d^{10} elements are not uncommon,[27] and their bonding character is usually derived from the hybridization effect.[28–30] These Cu–Cu distances are comparable with those ranging from 2.62 to 2.73 Å in the polytellurides $Ba_2Cu_{4-x}Se_yTe_{5-y}$,[14] as well as in $Ba_3Cu_{14-x}Te_{12}$[12] and $Ba_3Cu_{17-x}Se_yTe_{11-y}$,[19] where the bonding character was confirmed by calculations of their crystal orbital Hamilton populations.[31,32] Thus, the S/Se atoms, in part with Te contribution depending on the Se/Te ratio, are centering metal clusters with metal–metal bonds in $BaCu_{6-x}Q_{1-y}Te_{6+y}$.

The absence of any Se–Se contacts in $BaCu_{5.9}SeTe_6$ enables us to assign the 2– states to the Se atoms. This in turn then demonstrates the clear preference of Se for the position within the Cu_8 cubes, as the other chalcogen site bears a formal 1– charge, which will be less preferred for the more electronegative atom. Of course, the different steric requirements (smaller size of Se, compared to Te atoms) may also play a role here. Similarly, the S atoms are located on the isolated Q sites in $Ag_{12}Te_6S$ and not in the Te_2^{2-} dumbbells.[33]

Electronic Structure

We computed the electronic structures of three different models of the *BaCu$_6$SeTe$_6$* formula, with the SeCu$_6$ clusters as shown in Figure 2. Here in Figure 3 we only present the densities of states (DOS) and crystal orbital Hamilton population (COHP) curves of the averaged homonuclear bonds for the $R\bar{3}$ case, because the other models gave very similar densities of states and COHP curves (available as part of the Supporting Information). The most notable feature of this model is the presence of a small band gap at the Fermi level of approximately 0.05 eV, which is indicative of semiconducting properties for BaCu$_{6-x}$SeTe$_6$ with $x = 0$. This is in agreement with the charge-balanced *Ba^{2+}(Cu^{+})$_6$Se^{2-}(Te$_2^{2-}$)$_3$* formula, derived from the above-mentioned formal charges.

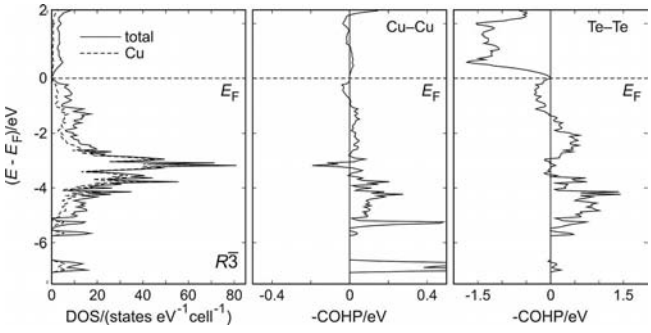

Figure 3. Densities of states (left) and averaged crystal orbital Hamilton populations of the Cu–Cu (center) and Te–Te bonds (right) of the *BaCu$_6$SeTe$_6$* model in space group $R\bar{3}$.

The valence band of *BaCu$_6$SeTe$_6$* extends from 0 eV down to –5.7 eV, and comprises Cu d and Te p states. The Se p states form the small peak around –6.8 eV, along with the Cu states, because of the covalent character of the Cu–Se bonds. The bottom of the conduction band is dominated by Te p states, which are Te–Te antibonding.

Analogous observations, namely that the bottom of the conduction band is composed of (empty) antibonding states originating from bonds between the chalcogen atoms, were also made for Sr$_2$SnSe$_5$,[34] Ba$_2$SnTe$_5$,[35] and Ba$_7$Cu$_2$Te$_{14}$.[13] It is concluded that the presence of polychalcogenide units favors narrower band gaps, which is advantageous for the thermoelectric energy conversion.[36,37]

The postulated bonding character for the Cu–Cu and Te–Te interactions becomes visible upon inspection of the respective COHP curves, because the filled bonding states clearly outnumber the filled antibonding states in both cases. In case of the Cu–Cu interactions, a large bonding contribution stems from the covalent mixing of the Cu and Se states, causing a strongly Cu–Cu bonding peak around –6.8 eV. Integrating over all filled states yields an integrated crystal orbital Hamilton population (ICOHP) value of –0.52 eV for the averaged Cu–Cu bond, comparable to the Cu–Cu bonds of similar lengths in Ba$_3$Cu$_{16}$Se$_8$Te$_3$ (–0.44 eV, 2.71 Å),[19] BaCu$_2$SnSe$_4$ (–0.32 eV, 2.70 Å), and in Ba$_3$Cu$_2$Sn$_3$Se$_{10}$ (–0.75 eV, 2.65 Å).[38] Shorter Cu–Cu bonds are known to occur in Ba-Cu chalcogenides, and are typically stronger (reflected in larger absolute ICOHP values), for example, the 2.46 Å bond with its ICOHP = –1.00 eV in Ba$_3$Cu$_{16}$Se$_8$Te$_3$.

The large ICOHP value of –1.97 eV of the Te–Te interaction in *BaCu$_6$SeTe$_6$* is indicative of a very strong bond, in agreement with the single bond character of the Te$_2^{2-}$ unit. This value compares well with the –1.98 eV for the 2.81 Å Te–Te bond in Ba$_2$SnTe$_5$.[35]

Physical Properties

The electronic structure calculations pointed to *p*-type semiconducting properties for BaCu$_{6-x}$Se$_{1-y}$Te$_{6+y}$ with $x > 0$. We determined the properties of phase-pure polycrystalline BaCu$_{5.7}$Se$_{0.6}$Te$_{6.4}$, that is, at the Te-rich end of the phase width, because tellurides typically have better thermoelectric properties than selenides. Assuming that all carriers stem solely from the Cu deficiency of 0.3 per formula unit, the carrier concentration can be estimated to be 8.8×10^{20} cm^{-3}, corresponding to a heavily doped material. Nevertheless, its electrical conductivity is rather low, with a room temperature value of $\sigma = 40\ \Omega^{-1}\,cm^{-1}$, and increases almost linearly with increasing temperature to just below $60\ \Omega^{-1}\,cm^{-1}$ at 573 K (white squares in Figure 4). This observation stands against such a higher number of itinerant extrinsic carriers as postulated above, indicating that some of these carriers may be localized. The increase in conductivity with increasing temperature may thus be caused by an increasing delocalization of the those charge carriers.

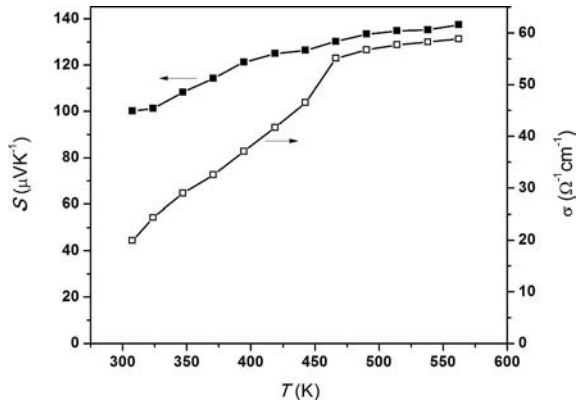

Figure 4. Seebeck coefficient (black squares) and electrical conductivity (white squares) of BaCu$_{5.7}$Se$_{0.6}$Te$_{6.4}$.

In parallel, the Seebeck coefficient increases from $S = +100$ to $+135\ \mu V\,K^{-1}$ (black squares in Figure 4), its positive numbers supporting the assumption of *p*-type conduction. These data are of the same magnitude as those obtained from single crystals of K$_2$BaCu$_8$Te$_{10}$ and Rb$_2$BaCu$_8$Te$_{10}$, with room-temperature values of $\sigma = 70\ \Omega^{-1}\,cm^{-1}$ and $S = +120\ \mu V\,K^{-1}$ for the former and $\sigma = 110\ \Omega^{-1}\,cm^{-1}$ and $S = +150\ \mu V\,K^{-1}$ for the latter.[39] The corresponding values for polycrystalline Ba$_3$Cu$_{13.88}$Te$_{12}$ are $\sigma = 190\ \Omega^{-1}\,cm^{-1}$ and $S = +35\ \mu V\,K^{-1}$.[12]

The thermal conductivity of $BaCu_{5.7}Se_{0.6}Te_{6.4}$, is very low, with values around $\kappa = 0.5\ W m^{-1} K^{-1}$ between 340 and 560 K (black squares in Figure 5), which is significantly lower than values for the other polytellurides: $1.1\ W m^{-1} K^{-1}$ for $Ba_3Cu_{13.88}Te_{12}$ and $1.2\ W m^{-1} K^{-1}$ for $Rb_2BaCu_8Te_{10}$. Part of the difference originates from its 15% porosity, and the significant mass fluctuations because of the 25% Cu atom deficiency and the Se/Te mixed occupancy are likely to play a major role, too.

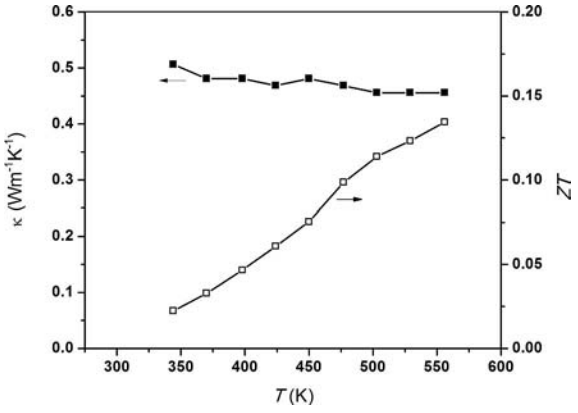

Figure 5. Thermal conductivity (black squares) and figure of merit (white squares) of $BaCu_{5.7}Se_{0.6}Te_{6.4}$.

The thermoelectric figure of merit, $ZT = TS^2\sigma/\kappa$, was obtained by using a polynomial fit for the power factor $P.F. = S^2\sigma$[40] and then calculating ZT from the fitted $P.F.$ and the measured κ values. ZT increases steadily from 0.02 at 340 K to 0.13 at 560 K (white squares in Figure 5). While larger values may be obtained by using better densified materials, these numbers are not competitive, noting that commercially used materials exhibit ZT values of the order of 1. Nevertheless, $BaCu_{5.7}Se_{0.6}Te_{6.4}$ performs better than the other barium copper chalcogenides, for example, $Ba_3Cu_{13.88}Te_{12}$ with its $ZT(320\ K) = 0.007$.

Conclusions

The new quaternary polychalcogenides, $BaCu_{6-x}STe_6$ and $BaCu_{6-x}Se_{1-y}Te_{6+y}$, adopt a hitherto unknown structure type, comprising chalcogen-centered Cu atom clusters and Te_2^{2-} dumbbells, while the Ba atoms are encapsulated in pentagonal Cu_8Te_{12} dodecahedra known from the structure of $A_2BaCu_8Te_{10}$ (A = K, Rb, Cs). The Cu deficiency, x, may vary within the range $0.04(2) \le x \le 0.28(2)$, and the Se content, $(1 - y)$, within $0.46(2) \le (1 - y) \le 1$. The hypothetical case with $x = 0$ is charge-balanced, $Ba^{2+}(Cu^{+})_6Se^{2-}(Te_2^{2-})_3$, and was calculated to be a narrow gap (intrinsic) semiconductor independent of the proposed Cu atom ordering. $BaCu_{5.7}Se_{0.6}Te_{6.4}$ was experimentally determined to be a p-type semiconductor with moderate thermoelectric figure of-merit, resulting from a combination of high Seebeck coefficient, low thermal conductivity, and too low electrical conductivity.

Experimental Section

Syntheses and Analyses

The elements were used for the syntheses as acquired: Ba pieces: 99% nominal purity, Sigma Aldrich; Cu powder: 99.9%, Alfa Aesar; S powder: 99.999%, Alfa Aesar; Se powder: 99.999%, Sigma Aldrich; Te powder: 99.8%, Sigma Aldrich (all stored in a glove box filled with argon). The quaternary selenide-telluride was first found when trying to prepare "$Ba_2Cu_{3.8}Se_{0.5}Te_{6.5}$". The reaction was carried out in a sealed silica tube by heating within six hours to 1073 K, followed by a slow cooldown to promote crystal growth over 200 h down to 573 K. Finally, the furnace was switched off. Because no known compound was detected in the X-ray powder diagram obtained from the ground reaction mixture, a single crystal was mounted on the Bruker Smart APEX to determine its crystal structure. As described below, that analysis identified a new compound: $BaCu_{5.72(2)}Se_{0.46(2)}Te_{6.54}$, which was obtained only in small yields.

Subsequently, a series of reactions was started in order to determine the phase width with respect to the Cu content as well as Se/Te ratio. Furthermore, we tried to replace Se with S. This series was prepared by first heating the elements in silica tubes up to 773 K within 24 h, followed by cooling down to 673 K within 200 h and finally to room temperature. Second, the samples were ground and annealed at 663 K for 240 h, because the yields of the target compounds were low before this step, which is possibly indicative of an incongruent melting point.

Phase-pure compounds, as determined by X-ray powder diffraction utilizing the Inel powder diffractometer with position-sensitive detector, were prepared when starting from: (a) 1 equiv. Ba, 5.9 equiv. Cu, 1 equiv. Se, 6 equiv. Te; (b) 1 equiv. Ba, 5.7 equiv. Cu, 0.5 equiv. Se, 6.5 equiv. Te; (c) 1 equiv. Ba, 5.9 equiv. Cu, 1 equiv. S, 6 equiv. Te. Increasing the Se concentration to 1.2 equiv. Se (and correspondingly 5.8 equiv. Te) led to the formation of side products, as did a further increase of Te to 6.75 equiv. Te (and Se to 0.25 equiv.). The same is true for increasing the Cu content above 5.9 equiv. or decreasing it below 5.7 equiv.

To probe the borders of the phase width more precisely, we determined the crystal structures (and thereby refined the formula) of three samples with side products, namely with $x = 5.4$ and 6.2 and $y = 1.2$ of the nominal composition $BaCu_{6-x}Se_{1-y}Te_{6+y}$. Moreover, one single crystal of each of the apparently phase-pure samples "$BaCu_{5.9}SeTe_6$" and "$BaCu_{5.9}STe_6$" was analyzed to verify the nominal formula. Including the first data collection, the refined formulas show a small phase range with respect to the Cu concentration [$0.04(2) \le x \le 0.28(2)$] and a larger one with respect to the Se content [$0.46(2) \le (1 - y) \le 1$], as summarized in Table 2.

Table 2. Refined formulas and CSD numbers of $BaCu_{6-x}Q_{1-y}Te_{6+y}$.

CSD No.	Starting ratio	Refined formula
422804	2 Ba/3.8 Cu/0.5 Se/6.5 Te	$BaCu_{5.72(2)}Se_{0.46(2)}Te_{6.54}$
422795	1 Ba/5.4 Cu/1 Se/6 Te	$BaCu_{5.89(3)}SeTe_6$
422794	1 Ba/5.9 Cu/1 Se/6 Te	$BaCu_{5.93(2)}SeTe_6$
422797	1 Ba/6.2 Cu/1 Se/6 Te	$BaCu_{5.92(2)}Se_{0.96(1)}Te_{6.04}$
422798	1 Ba/5.9 Cu/1.2 Se/5.8 Te	$BaCu_{5.96(2)}SeTe_6$
422796	1 Ba/5.9 Cu/1 S/6 Te	$BaCu_{5.92(2)}S_{0.986(4)}Te_{6.014}$

Energy-dispersive analysis of X-rays using an electron microscope (LEO 1530) with an additional EDX device (EDAX Pegasus 1200) did not show any heteroelements for the sample of nominal composition $BaCu_{5.6}Se_{0.6}Te_{6.4}$. Averaged over eight crystals, the Ba/Cu/Se/Te ratio was obtained to be 7.6:44.1:6.6:41.7, while a smaller Se

Table 3. Crystallographic details of $BaCu_{6-x}Q_{1-y}Te_{6+y}$.

Refined formula	$BaCu_{5.72(2)}Se_{0.46(2)}Te_{6.54}$	$BaCu_{5.93(2)}SeTe_6$	$BaCu_{5.92(2)}S_{0.986(4)}Te_{6.014}$
Formula weight (g/mol)	1371.61	1358.69	1312.49
T of measurement (K)	296(2)	296(2)	296(2)
λ (Å)	0.71073	0.71073	0.71073
Space group	$Pm\bar{3}$	$Pm\bar{3}$	$Pm\bar{3}$
a (Å)	6.9888(4)	6.9680(2)	6.9266(5)
V (Å^3)	341.36(3)	338.32(2)	332.32(4)
Z	1	1	1
μ (mm^{-1})	26.45	27.32	25.25
$\rho_{calcd.}$ (g/cm^3)	6.37	6.67	6.56
Total, independent, observed reflections (R_{int})	4024, 216, 213 (0.028)	1940, 205, 201 (0.024)	3640, 204, 203 (0.030)
$R(F_o)\backslash R_w(F_o^2)$[a] all data	0.011 \ 0.027	0.011 \ 0.023	0.011 \ 0.036

[a] $R(F_o) = \Sigma||F_o| - |F_c||/\Sigma|F_o|$; $R_w(F_o^2) = \{\Sigma[w(F_o^2 - F_c^2)^2]/\Sigma[w(F_o^2)^2]\}^{1/2}$.

content was expected, according to the atom-% derived from the nominal formula Ba/Cu/Se/Te = 7.4:41.2:4.4:47.1. The difference may be due to difficulties when determining the concentration of any element below 10%.

A differential scanning calorimetry measurement was performed on the $BaCu_{5.9}SeTe_6$ sample under a flow of argon with the Netzsch STA 409PC Luxx as described before.[38] This experiment showed an incongruent melting point of $BaCu_{5.9}SeTe_6$ to be at 718 K (figure available as part of the Supporting Information), as the sample was decomposed into binary and ternary chalcogenides during this experiment.

Single-crystal X-ray diffraction data were collected by using a Bruker Smart Apex CCD diffractometer that employs Mo-K_α radiation at room temperature. Scans of 0.3° in ω were performed at three different ϕ angles with exposure times of 30 seconds each for a total of 2×600 frames in the first case (initial composition "$Ba_2Cu_{3.8}Se_{0.5}Te_{6.5}$"). The data collected in this way were treated for Lorentz and polarization corrections. The absorption corrections were based on fitting a function to the empirical transmission surface as sampled by multiple equivalent measurements. The APEX II package,[41] which includes the SHELXTL program package,[42] was used for the data reduction and structure refinement.

The lattice parameters pointed towards a cubic primitive lattice, and the internal R value of 56.6% for the $m3m$ Laue group along with the absence of any systematic extinctions restricted the possible space groups to $P23$ and $Pm\bar{3}$, with $R_{int} = 2.1\%$. Because the structure refinements gave virtually the same results in these two space groups, the higher symmetry, $Pm\bar{3}$, was chosen as the final space group.

Applying the direct methods in $Pm\bar{3}$ yielded four positions, which were readily assigned as one Ba (on Wyckoff site 1b), one Cu (8i), one Te (6f), and one Se (1a) site. Refining this model of $BaCu_8SeTe_6$ yielded $R(F_o) = 0.066$ (all reflections) and a high U_{eq} of the Cu site of 0.046 Å^2. Refining the occupancy of Cu significantly lowered $R(F_o)$ from 0.066 to 0.026, and the occupancy to 70% and U_{eq} to 0.026 Å^2. To address the electron density maximum of 4.4 e Å^{-3} located at a distance of 0.38 Å to the Se site (noting that the deepest hole was only 0.8 e Å^{-3}), we refined that site as mixed occupied by Se and Te (called Se2/Te2). This further lowered $R(F_o)$, namely from 0.026 to 0.011, and yielded a Se/Te ratio of 46:54 on that site, and thus ultimately a refined formula of $BaCu_{5.72(2)}Se_{0.46(2)}Te_{6.54}$. This refinement occurred with an enlarged U_{eq} value of the Se2/Te2 site of 0.056 Å, most likely because the Se and Te atoms prefer different locations within the disordered Cu cluster. Finally, the Te1 site (6f) was tentatively refined as a Se/Te mixture, which resulted in no Se content on that site. Thus, the 6f site was considered to be exclusively Te.

Five more data collections, listed in Table 2, were carried out in order to determine the phase width both with respect to x and y of $BaCu_{6-x}Se_{1-y}Te_{6+y}$ as well as to prove the existence of the isostructural sulfide-telluride. In each case, the Cu occupancy was refined, and the chalcogen sites were tentatively treated as mixed occupied. In each case, the Cu occupancy was below 75%, and the occupancy of the 6f site was always equal to 100% within one standard deviation. When the deviation from full occupancy was within twice its standard deviation, the site was refined as fully occupied in the final refinement. Because no evidence was found for an incorporation of Se on the Te2 site, it is concluded that y cannot exceed 1 significantly. No diffuse scattering was observed, and tentative refinements in space groups of lower symmetry (see below) revealed no ordering of the defects.

Selected crystallographic details are given in Table 3. Atomic positions of $BaCu_{5.93(2)}SeTe_6$ are listed in Table 4. Further details of the crystal structure investigation can be obtained from the Fachinformationszentrum Karlsruhe, 76344 Eggenstein-Leopoldshafen, Germany, [Fax: +49-7247-808-666; E-mail: crysdata@fiz-karlsruhe.de] on quoting the various depository numbers (CSD 422794–422798 and 422804) as detailed in Table 2.

Table 4. Atomic coordinates, equivalent isotropic displacement parameters, and occupancy factors of $BaCu_{5.93(2)}SeTe_6$.

Atom	Site	x	y	z	U_{eq} (Å^2)
Ba	1b	1/2	1/2	1/2	0.0195(1)
Cu[a]	8i	0.19935(5)	x	x	0.0235(2)
Te1	6f	0.30033(3)	0	1/2	0.0159(1)
Se2	1a	0	0	0	0.0241(2)

[a] Occupancy 0.741(2).

Electronic Structure Calculations

The structural parameters from the refinement of $BaCu_{5.93(2)}SeTe_6$ were used as basis for the calculation. To model the Cu deficiency, three different models of formula *BaCu$_6$SeTe$_6$* were considered with different, hypothetical Cu atom ordering, leading to three different space groups, namely $R\bar{3}$, Pm, and $P2$ (Figure 2).

The DFT-based LMTO method (linear muffin tin orbitals), which utilizes the atomic spheres approximation (ASA), was employed for all computations.[43,44] In the LMTO approach, the density functional theory is used with the local density approximation (LDA) to approximate the exchange-correlation energy functional.[45] Depending on the symmetry, grids of 294 to 1008 independent k points of the first Brillouin zone were chosen for the integrations in k space by an improved tetrahedron method.[46]

Measurements of Physical Properties

Phase-pure $BaCu_{5.7}Se_{0.6}Te_{6.4}$ was chosen for measuring the physical properties. By pressing at approximately 600 MPa, a density of 85% of the theoretical maximum was obtained. The electronic transport properties, Seebeck coefficient (S), and electrical conductivity (σ) were simultaneously measured under helium by utilizing a ULVAC-RIKO ZEM-3 instrument between room temperature and 573 K. Thermal diffusivity (α) was determined under argon with the Anter Flashline™ 3000 between 340 and 560 K. The sample exhibited no sign of decay after either process. Thermal conductivity (κ) was calculated by the formula $\kappa = \rho\alpha C_P$, with ρ = density, and C_P was taken from the Dulong–Petit law. ZT values were calculated from a polynomial fit of the power factor ($S^2\sigma$) and the κ values into $ZT = TS^2\sigma/\kappa$.

Supporting Information (see footnote on the first page of this article): Thermal analysis of $BaCu_{5.9}SeTe_6$, and densities of states and averaged crystal orbital Hamilton populations of the Cu–Cu and Te–Te bonds of the $BaCu_6SeTe_6$ models in space group Pm and $P2$.

Acknowledgments

Financial support from the Natural Sciences and Engineering Research Council and the Canada Research Chair program (CRC for H. K.) is appreciated.

[1] J.-M. Tarascon, M. Armand, *Nature* **2001**, *414*, 359–367.
[2] R. Venkatasubramanian, E. Slivola, T. Colpitts, B. O'Quinn, *Nature* **2001**, *413*, 597–602.
[3] H. Xu, K. M. Kleinke, T. Holgate, H. Zhang, Z. Su, T. M. Tritt, H. Kleinke, *J. Appl. Phys.* **2009**, *105*, 053703/053701–053703/053705.
[4] M. G. Kanatzidis, *Chem. Mater.* **2010**, *22*, 648–659.
[5] G. Atwood, *Science* **2008**, *321*, 210–211.
[6] D. Lencer, M. Salinga, B. Grabowski, T. Hickel, J. Neugebauer, M. Wuttig, *Nat. Mater.* **2008**, *7*, 972–977.
[7] N. Yamada, M. Wuttig, *Nat. Mater.* **2007**, *6*, 824–832.
[8] X. Ji, K. T. Lee, L. F. Nazar, *Nat. Mater.* **2009**, *8*, 500–506.
[9] N. D. Lowhorn, T. M. Tritt, E. E. Abbott, J. W. Kolis, *Appl. Phys. Lett.* **2006**, *88*, 022101/022101–022101/022103.
[10] T. Nilges, S. Lange, M. Bawohl, J. M. Deckwart, M. Jansen, H.-D. Wiemhöfer, R. Decourt, B. Chevalier, J. Vannahme, H. Eckert, R. Weihrich, *Nat. Mater.* **2009**, *8*, 101–108.
[11] A. Assoud, J. Xu, H. Kleinke, *Inorg. Chem.* **2007**, *46*, 9906–9911.
[12] A. Assoud, S. Thomas, B. Sutherland, H. Zhang, T. M. Tritt, H. Kleinke, *Chem. Mater.* **2006**, *18*, 3866–3872.
[13] Y. Cui, A. Assoud, J. Xu, H. Kleinke, *Inorg. Chem.* **2007**, *46*, 1215–1221.
[14] O. Mayasree, Y. Cui, A. Assoud, H. Kleinke, *Inorg. Chem.* **2010**, *49*, 6518–6524.
[15] H. Schäfer, B. Eisenmann, W. Müller, *Angew. Chem.* **1973**, *85*, 742; *Angew. Chem. Int. Ed. Engl.* **1973**, *12*, 694–712.
[16] R. Nesper, *Prog. Solid State Chem.* **1990**, *20*, 1–45.
[17] S. M. Kauzlarich, *Chemistry, Structure, and Bonding of Zintl Phases and Ions: Selected Topics and Recent Advances*, VCH Publishers, New York, **1996**.
[18] J. D. Corbett, *Angew. Chem.* **2000**, *112*, 682; *Angew. Chem. Int. Ed.* **2000**, *39*, 670–690.
[19] B. Kuropatwa, Y. Cui, A. Assoud, H. Kleinke, *Chem. Mater.* **2009**, *21*, 88–93.
[20] O. Mayasree, C. R. Sankar, A. Assoud, H. Kleinke, *Inorg. Chem.* **2011**, *50*, 4580–4585.
[21] S. Debus, B. Harbrecht, *Z. Anorg. Allg. Chem.* **2001**, *627*, 431–438.
[22] B. C. Guo, K. P. Kerns, A. W. Castleman Jr., *Science* **1992**, *255*, 1411–1413.
[23] Y. Park, M. G. Kanatzidis, *Chem. Mater.* **1991**, *3*, 781–783.
[24] X. Zhang, Y. Park, T. Hogan, J. L. Schindler, C. R. Kannewurf, S. Seong, T. Albright, M. G. Kanatzidis, *J. Am. Chem. Soc.* **1995**, *117*, 10300–10310.
[25] P. Böttcher, J. Getzschmann, R. Keller, *Z. Anorg. Allg. Chem.* **1993**, *619*, 476–478.
[26] R. J. Batchelor, F. W. B. Einstein, I. D. Gay, C. H. W. Jones, R. D. Sharma, *Inorg. Chem.* **1993**, *32*, 4378–4383.
[27] M. Jansen, *Angew. Chem.* **1987**, *99*, 1136; *Angew. Chem. Int. Ed. Engl.* **1987**, *26*, 1098–1110.
[28] P. K. Mehrotra, R. Hoffmann, *Inorg. Chem.* **1978**, *17*, 2187–2189.
[29] K. M. Merz Jr., R. Hoffmann, *Inorg. Chem.* **1988**, *27*, 2120–2127.
[30] P. Pyykkö, *Chem. Rev.* **1997**, *97*, 597–636.
[31] R. Dronskowski, P. E. Blöchl, *J. Phys. Chem.* **1993**, *97*, 8617–8624.
[32] G. A. Landrum, R. Dronskowski, *Angew. Chem.* **2000**, *112*, 1598; *Angew. Chem. Int. Ed.* **2000**, *39*, 1560–1585.
[33] H. Mikus, H. J. Deiseroth, *Z. Anorg. Allg. Chem.* **2005**, *631*, 1233–1236.
[34] A. Assoud, N. Soheilnia, H. Kleinke, *Chem. Mater.* **2004**, *16*, 2215–2221.
[35] A. Assoud, S. Derakhshan, N. Soheilnia, H. Kleinke, *Chem. Mater.* **2004**, *16*, 4193–4198.
[36] J. O. Sofo, G. D. Mahan, *Phys. Rev. B* **1994**, *49*, 4565–4570.
[37] J. Xu, H. Kleinke, *J. Comput. Chem.* **2008**, *29*, 2134–2143.
[38] A. Assoud, N. Soheilnia, H. Kleinke, *Chem. Mater.* **2005**, *17*, 2255–2261.
[39] R. Patschke, X. Zhang, D. Singh, J. Schindler, C. R. Kannewurf, N. Lowhorn, T. Tritt, G. S. Nolas, M. G. Kanatzidis, *Chem. Mater.* **2001**, *13*, 613–621.
[40] D. M. Rowe, *CRC Handbook of Thermoelectrics*, CRC Press, Boca Raton, FL, **1995**.
[41] *M86-Exx078 APEX2 User Manual*, Bruker AXS Inc., Madison, WI, **2006**.
[42] G. M. Sheldrick, *Acta Crystallogr., Sect. A* **2008**, *64*, 112–122.
[43] O. K. Andersen, *Phys. Rev. B* **1975**, *12*, 3060–3083.
[44] H. L. Skriver, *The LMTO Method*, Springer, Berlin, Germany, **1984**.
[45] L. Hedin, B. I. Lundqvist, *J. Phys. C* **1971**, *4*, 2064–2083.
[46] P. E. Blöchl, O. Jepsen, O. K. Andersen, *Phys. Rev. B* **1994**, *49*, 16223–16233.

Received: March 21, 2011
Published Online: May 26, 2011

